ELSEVIER

Contents lists available at ScienceDirect

# **Chemical Geology**

journal homepage: www.elsevier.com/locate/chemgeo





# Measurement of total amine site concentrations on bacterial cell surfaces using selective site-blocking and potentiometric titrations

Qiang Yu\*, Jeremy B. Fein

Department of Civil & Environmental Engineering & Earth Sciences, University of Notre Dame, Notre Dame, Indiana 46556, United States

#### ARTICLE INFO

Editor:Dr. Hailiang Dong

Keywords:
Potentiometric titration
Amine
Bacterial cell surface
Surface complexation modeling

#### ABSTRACT

Bacterial cell surface amine binding sites can form strong complexes with both toxic metal cations and anionic contaminants, thereby affecting the behavior of these contaminants in both natural and engineered systems. In this study, a novel approach was developed to measure the concentration of total amine sites on bacterial cell surfaces by combining selective site-blocking, potentiometric titrations and surface complexation modeling. Our controls show that the amine blocker sulfo-N-hydroxysulfosuccinimide acetate (SNHS) selectively reacts with primary and secondary amine sites but does not react with other binding sites on the bacterial cell surface. Amine site concentrations on bacterial cell surfaces, therefore, can be measured as the difference between the total site concentrations of un-blocked and SNHS-blocked bacterial samples. We measured amine site concentrations on Bacillus subtilis and Pseudomonas putida of  $52 \pm 5$  and  $78 \pm 6$  µmol/g, respectively, which account for 24% and 32% of the total binding sites on each bacterial surface. Our results suggest that amine sites can be present in relatively high concentrations on bacterial surfaces, and further studies that are focused on the role of cell surface amine sites on the transport and bioavailability of toxic metal cations and anionic contaminants are crucial.

### 1. Introduction

Bacteria are ubiquitous in the environment and can control element cycling and the mobility and fate of soil and groundwater contaminants through adsorption, reduction/oxidation, and/or degradation reactions (Beveridge and Murray, 1976; Lovley, 1993; Fuchs et al., 2011). The organic acid functional groups on bacterial cell surfaces play an important role in these processes because adsorption onto these binding sites typically represents the first step of solute-bacteria interaction. For example, bacterial surface binding sites not only directly control the adsorption of a variety of metals such as Cd, Zn and Hg onto bacterial cells (Beveridge and Murray, 1976; Daughney et al., 2002; Guiné et al., 2006), but also contribute to bacterial reduction of a range of elements such as Au, Se and Cr (Kang et al., 2017; Yu et al., 2018; Brown et al., 2024). Previous research has highlighted the important role of carboxyl, phosphoryl, amine and sulfhydryl binding site types on bacterial cell surfaces (Fein et al., 1997; Cox et al., 1999; Ngwenya et al., 2003; Jiang et al., 2004; Guiné et al., 2006; Brown et al., 2024). In order to understand and model the role of these sites in bacterially-controlled reactions, it is crucial to determine which surface sites are involved and to measure their cell surface abundance and reactivity.

Bacterial cell surface amine binding sites have been identified as potentially important in a range of microbe-mediated reactions. For example, amine binding can control aqueous metal cation adsorption onto bacterial cells (Beveridge and Murray, 1980; Chang et al., 2023), Zn uptake by some plants (Mishra et al., 2020), and Cr(VI) reduction by bacteria (Brown et al., 2024). Although the total concentration of binding sites on bacterial cell surfaces and the concentration of some specific types of binding sites (e.g., sulfhydryl) have been measured (Beveridge and Murray, 1980; Joe-Wong et al., 2012; Yu et al., 2014), measurements of the concentration of amine binding sites are scarce. Beveridge and Murray (1980) used an indirect molecular tagging approach to quantify amine site concentrations on isolated Bacillus subtilis bacterial cell walls, measuring approximately 0.3 µmol of sites/g cell wall, but this is the only published amine site concentration measurement, and it is difficult to use this value to determine the absolute and relative concentration of amine sites on undisturbed whole cells.

Amine sites are distinct from the other bacterial surface functional groups in that they are positively charged when protonated and neutrally charged when deprotonated. In their neutral state, amine sites can complex with metal cations (Eßmann, 1995; Modec et al., 2020), and when they are positively charged, amine sites can bind negatively

<sup>\*</sup> Corresponding author.

E-mail address: qyu@nd.edu (Q. Yu).

charged solutes (Deng et al., 2008; Deng et al., 2009; Deng et al., 2013). Because of their positive charge when protonated, amine sites likely play an important role in the adsorption of, and bacterial reactivity with, anionic metalloids (e.g., chromate (Srinath et al., 2002), arsenate (Tariq et al., 2019), etc.) and anionic organic molecules (e.g., deprotonated PFAS molecules (Butzen and Fein, 2020), etc.). In order to fully understand and model the role of amine sites in bacterial interactions with metals, metalloids, and anionic solutes, it is crucial to quantify the concentrations of amine sites on bacterial cell surfaces.

Currently, the best available method to measure the total concentration of proton-active binding sites on bacterial cell surfaces is an approach that combines potentiometic titration and surface complexation modeling (SCM) (Xue et al., 1988; Fein et al., 1997; Cox et al., 1999; Pagnanelli et al., 2000; Ngwenya et al., 2003; Yee et al., 2004). Although this approach provides a reliable means to derive total site concentrations, and has been used effectively to constrain the protonation behavior of cell envelope functional groups (Daughney and Fein, 1998; Ngwenya et al., 2003; Takahashi et al., 2005), the interpretation of the data to infer concentrations and acidity constant  $(pK_a)$  values for specific proton-active binding sites is model-dependent (Fein et al., 2005a). The potentiometric titration approach models the measured buffering behavior of bacterial cells by solving for  $pK_a$  values and associated site concentrations, defining a site not as an entity having a specific chemical composition, but rather as the set of functional groups that have the same  $pK_a$  value. Because different chemical functional group types (e.g., carboxyl, phosphoryl, amine, etc.) can have similar  $pK_a$  values, this approach does not directly constrain the concentration of each chemical type of functional group on bacterial cell surfaces. In order to quantify the concentration of sulfhydryl sites on bacterial cell surfaces, we previously developed a method that couples selective blocking of sulfhydryl sites with potentiometric titrations and surface complexation modeling (Yu et al., 2014), precisely measuring the total available site concentrations with and without sulfhydryl-specific blocking. In this approach, the difference in these measured total site concentrations equals the concentration of sulfhydryl sites on the cell surface. This site-blocking approach can be extended to measure the concentrations of other types of bacterial surface sites if appropriate site-specific blockers are available.

In this study, we use a site-specific blocking approach to measure the concentration of amine sites on bacterial cell surfaces. We use a commercially available amine blocker, sulfo-Nhydroxysulfosuccinimide acetate (SNHS), for selectively blocking amine sites. We first demonstrate the amine-selectivity and reactivity of SNHS using silica resins coated with different types of functional groups. We then use potentiometric titrations and surface complexation modeling to determine the concentration of total binding sites present within suspensions of bacterial cells with and without SNHS treatment of the cells to block the amine sites. The concentration of amine sites is determined by measuring the decrease in the concentration of total binding sites after the amine sites were selectively blocked by SNHS. Using this approach, we report the concentrations of amine sites on bacterial cell surfaces of a Gram-negative (Pseudomonas putida) and a Gram-positive (Bacillus subtilis) bacterial species, both of which are widely found in soil and water.

# 2. Materials and Methods

#### 2.1. Materials

Sulfo-N-hydroxysulfosuccinimide acetate (SNHS) and L-cysteine (CYS) were purchased from Thermo Fisher Scientific, Inc. and Sigma Aldrich, Inc., respectively. Five silica-based resins with different functional group coatings were used in this study to test the selectivity of SNHS. Their manufacturers and properties are shown in Table 1. The Si-Thiol and Si-Carboxyl resins were used to simulate the sulfhydryl and carboxyl sites on bacterial cell surfaces, respectively. Two Si-Trisamine

 Table 1

 Properties of Silica-based Resins (manufacturer's data).

Resin	Manufacturer	Functional Groups	Catalogue #
Si-Thiol	Biotage	-SH	9180-0010
Si-Carboxyl	Silicycle	-COOH	R70030B-5G
Si-Sulfonic	Biotage	-SO <sub>3</sub> H	9536-0010
Si-TrisamineB*	Biotage	-NH/NH <sub>2</sub> (1:2)	9450-0010
Si-TrisamineS*	Supra Sciences	-NH/NH <sub>2</sub> (2:1)	SPSI20-25

 $<sup>^{\</sup>ast}$  Here 'B' designates the trisamine resin from Biotage and 'S' the trisamine resin from Supra Sciences.

resins that contain different ratios of primary( $-NH_2$ )/secondary(-NH) amine sites were used to test the reactivity of SNHS towards the two different amine site types. The Si-Sulfonic resin whose sulfonic sites have a  $pK_a < 2$  was used as a control to measure the buffering capacity of the silica base of the resins. Each of the resins was used as received.

#### 2.2. Bacterial Cell Preparation

One Gram-negative (Pseudomonas putida) and one Gram-positive (Bacillus subtilis) bacterial species were studied. The procedures for growth and washing of the bacterial cells were similar to those described previously (Fein et al., 1997; Fein et al., 2005a). Briefly, cells of each bacterial species were first cultured aerobically in 3 mL of autoclaved trypticase soy broth with 0.5% yeast extract at 32  $^{\circ}\text{C}$  for 24 h and then transferred to 2 L of autoclaved growth medium of the same composition at 32 °C for another 24 h. After incubation with agitation (100 rpm), the bacterial cells were harvested by centrifugation at 10,970g for 5 min. The biomass pellets were rinsed with a 0.1 M NaCl solution, followed by centrifugation at 8100g for 5 min, and the same process was repeated three times. The biomass pellets were then transferred into pre-weighed test tubes and centrifuged for two 30-min intervals at 8100g. After decanting the supernatant, this wet weight of the cells was used to calculate the bacterial concentrations in the subsequent experiments, and the bacterial concentrations that are reported in this study are these wet weights.

#### 2.3. Blocking of Amine Sites

In order to block amine sites on the cell and resin surfaces, the bacterial pellets or resins were suspended in a freshly prepared SNHS solution in 0.1 M NaCl with pH buffered to 8.5  $\pm$  0.1 using a 1.8 mM Na<sub>2</sub>HPO<sub>4</sub>/18.2 mM NaH<sub>2</sub>PO<sub>4</sub> buffer, with a SNHS:solid ratio of 0.2 mmol/g for the biomass samples and 8 mmol/g for the resins. We attempted to use enough SNHS to attain a 2:1 M ratio for SNHS: amine sites for each sample in order to completely block all the amine sites. Our results (shown in Tables 2 and 4) indicate that the added SNHS concentration was actually approximately 3-4 times the measured amine site concentrations on the biomass samples, and 6-7 times the measured amines site concentrations on the amine resins. Therefore, we conclude that the added SNHS concentration during the pre-treatment was sufficient to block all of the amine sites on each type of surface studied. Each mixture was allowed to react for 2 h at room temperature under continuous shaking on a rotating plate at 60 rpm. The manufacturer's instructions suggest 1 h of reaction time (ThermoScientific, 2023), so a 2 h soak time should be sufficient for the blocking reaction to be completed. We also tested a 3 h soak time, and we did not find a difference in the titration results between the 2 h and 3 h soak time samples (data not shown). After the reaction, the biomass or resin bead pellets were separated from the SNHS solution by centrifugation at 8100 g for 5 min. The pellets were rinsed with a 0.1 M NaCl solution, followed by centrifugation at 8100 g for 5 min, and the same wash process was repeated three times. The biomass or resin pellets were then transferred into pre-weighed test tubes and centrifuged for two 30-min intervals at 8100 g. After decanting the supernatant, the wet weight of the cells or

 Table 2

 Calculated individual and total site concentrations for the resins using a two-site SCM.

Resin	Treatment	Site1	Site1		Site2	
		pK <sub>a</sub>	Conc (mmol/g)	pK <sub>a</sub>	Conc (mmol/g)	(mmol/g)
Ci Tuissasia o	Untreated	$4.3\pm0.1$	$0.20\pm0.00$	$8.9 \pm 0.1$	$0.86\pm0.07$	$1.09\pm0.02$
Si-TrisamineS	SNHS-treated	$5.4\pm0.0$	$0.10\pm0.00$	$9.4\pm0.0$	$0.18\pm0.04$	$0.28\pm0.04$
Ci Tuissania sp	Untreated	$6.6\pm0.3$	$0.31\pm0.05$	$9.0\pm0.0$	$0.92\pm0.04$	$1.23\pm0.01$
Si-TrisamineB	SNHS-treated	$5.2\pm0.2$	$0.12\pm0.01$	$9.1\pm0.1$	$0.21\pm0.01$	$0.33\pm0.02$
Si-Sulfonic	Untreated	$4.8\pm1.6$	$0.03\pm0.01$	$9.6 \pm 0.3$	$0.30\pm0.04$	$0.32\pm0.03$

The values shown are averages with associated 1σ uncertainties from triplicate titrations.

resin was recorded.

#### 2.4. Potentiometric Titrations

Potentiometric titrations were conducted using a T70 autotitrator from Mettler Toledo Inc. and using 1 M HCl or NaOH calibrated standards purchased from Fluka Chemical Corp. Prior to each titration, the 0.1 M NaCl solution in which the titration was to be conducted was purged with N<sub>2</sub> gas for at least 1 h in order to remove dissolved CO<sub>2</sub>, and the electrode for pH measurement was calibrated using NIST-derived standard buffer solutions with pH values of 1.68, 4.01, 7.00 and 10.01. Bacterial cells with or without SNHS treatment were then suspended in the degassed 0.1 M NaCl solution to achieve a homogeneous suspension with a bacterial concentration of approximately 30 g/L, and 10-11 mL of this suspension was used in each titration. Titrations of resin-bearing suspensions were conducted using the same procedure as was used for the biomass samples except that we used a resin concentration of 5 g/L. In order to test the accuracy of the potentiometric titration approach for measuring amine sites, some titrations were conducted without suspended solids, titrating 0.1 M NaCl alone, 0.1 M NaCl with 1 mM CYS, and 0.1 M NaCl with 1 mM CYS and 1 mM monobromo(trimethylammonio)bimane bromide (qBBr, supplied by Toronto Research Chemical, Inc.). A CYS molecule has three functional groups: carboxyl, amine and sulfhydryl groups, with  $pK_a$  values of 1.92, 8.37 and 10.70, respectively (O'Neil, 2013). Therefore, the buffering capacity of a CYS solution in a pH range of 3.0-9.7 is primarily due to the deprotonation of the amine group, but is slightly affected by the protonation of the sulfhydryl sites as well. The qBBr molecule selectively blocks the sulfhydryl sites on CYS (Yu et al., 2014), so our titrations of the 1 mM CYS solution that also contained 1 mM qBBr solution were conducted to isolate the buffering behavior of the amine sites alone. All of the titrations were conducted in a closed vessel with N2 gas continuously supplied to the headspace, and each suspension or titrated solution was stirred continuously with a teflon-coated magnetic stir bar.

For each titration, two steps were conducted: 1) acidifying the suspension or solution from the original pH down to pH 3.0 by adding HCl standard; and 2) an up-pH titration from pH 3.0 to pH 9.7 by adding NaOH standard. Only these up-pH titration data were used for the surface complexation modeling to calculate the total amine site concentrations. The autotitrator was set to operate using a method in which the equilibration time for each step of the titration was controlled, and the volume of acid or base added at each step was recorded, with a minimum addition volume of 0.25  $\mu$ L. New titrant was added after the signal drift reached a minimum stability of 0.01 mV/s, or after a maximum waiting time of 60 s was achieved. In preliminary experiments, we conducted down-pH titrations from pH 9.7 to pH 3.0 immediately following the up-pH titrations, and the obtained titration curves (not shown) matched well with their corresponding up-pH titrations, suggesting rapid reversibility of the protonation reactions and that no significant damage occurred to the cells or resins during the up-pH titrations. The total titrant addition during the two titration steps caused the ionic strength of the experiments to increase only from 0.100 M to ~0.115 M, and this small change in ionic strength is accounted for in our surface complexation modeling by activity coefficient calculations (see

below).

In order to compare titration results from different experiments involving bacteria, the results were plotted in terms of a mass normalized net concentration of protons added to the system:

$$[\mathrm{H}^{+}]_{\mathrm{net\ added}} = (\mathrm{C_a} - \mathrm{C_b})/m \tag{1}$$

where  $C_a$  and  $C_b$  are the total concentrations of acid and base added to the system during the titration, respectively, with units of mmol/L of biomass suspension, and m is the bacterial concentration in the suspension, with units of g/L. The resin experimental results were not mass normalized because each experiment involved identical masses of resin. For each sample, triplicate titration experiments were conducted using three separately prepared suspensions of the same biomass or resin sample, and the reported site concentrations represent the averages of the triplicates with their associated  $1\sigma$  uncertainties.

# 2.5. Surface Complexation Modeling

In our surface complexation modeling approach, we assume that the proton-active functional groups on bacterial cell surfaces or on resin surfaces are discrete mono-protic acids, whose deprotonation reactions can be expressed using the following reaction (Fein et al., 2005b):

$$R - A_i H^{\circ} \leftrightarrow R - A_i^- + H^+ \tag{2}$$

where R denotes the bacterial envelope or resin surface macromolecule to which the  $i^{th}$  organic acid functional group,  $A_i$ , is attached. Note that although we write Reaction (2) here for an organic acid functional group, the same approach applies to protonation of amine-type sites as long as they are proton-active, and the actual charge of the protonated and deprotonated forms of the sites do not affect the calculations in the non-electrostatic surface complexation model that we used. The acidity constant  $(K_{a,i})$  and the total concentration  $(C_i)$  of the  $i^{th}$  site can be expressed as:

$$K_{a,i} = \frac{[R - A_i^{-}]a_{H^+}}{[R - A_i H^0]}$$
 (3)

$$C_i = [R - A_i^{-}] + [R - A_i H^0]$$
(4)

where  $[R-A_i^-]$  and  $[R-A_iH^0]$  represent the concentrations of the deprotonated and protonated  $i^{th}$  organic acid functional group on the bacterial cell envelope, respectively, and  $a_{H^+}$  is the activity of  $H^+$  in the bulk solution.

Based on proton mass balance, the concentration of protons added to the system at any point of the titration can be described as:

$$C_{a} - C_{b} = [H^{+}] - T_{H}^{0} - [OH^{-}] - \sum_{i} [R - A_{i}^{-}]$$
(5)

where  $T_H^0$  represents the initial proton concentration at the commencement of the titration, [X] represents the concentration of species X in the experimental system, including  $H^+$ ,  $OH^-$  and all the deprotonated organic acid functional groups on the bacterial cell surface or on the resin surface.

FITEQL (Westall, 1982) was used as a modeling tool for optimization

of  $T_{H}^{0}$ ,  $K_{a,i}$  and  $C_{i}$  in Eqs. (3), (4) and (5) to best fit the titration data and to solve for these unknown parameters, following the approach described by Fein et al. (Fein et al., 2005b) Activity coefficients of aqueous species were computed from the Davies equation within the FITEQL program (Westall, 1982). In our previous studies (Yu et al., 2014), we attempted to use one-, two-, three-, and four-site models to fit potentiometric titration data for bacterial suspensions, finding that a four-site non-electrostatic model yields the best fit to the titration data for each of the bacterial species considered. The same four-site approach was used in the present study to fit the titration data and in order to determine total binding site concentrations. Therefore, the concentration of total binding sites ( $C_{total}$ ) on bacterial cell surfaces can be calculated as:

$$C_{\text{total}} = C_1 + C_2 + C_3 + C_4 \tag{6}$$

where  $C_1$ ,  $C_2$ ,  $C_3$ ,  $C_4$  represent the total concentrations for each of the four site types described by the four-site model, respectively. Here, we refer to a 'site type' as a binding site with a specific  $pK_a$  value rather than one with a specific chemical formula, and hence each site type may contain binding sites with different chemical identities. Following this approach means that a specific chemical identity (e.g., carboxyl, amine, etc.) should not be assigned to what we refer to as a 'site type' with a specific  $pK_a$  value.

In order to calculate the concentration of amine sites in a sample, three titration experiments were conducted for each solid (bacteria or resin) with and without SNHS treatment. We used the Student's t-test to determine if the concentration of total binding sites decreased significantly after SNHS treatment, with a P value <0.05 taken to indicate a significant difference between the total site concentrations from the samples with and without SNHS treatment. The amine site concentration for each bacterial biomass sample ( $C_{amine}$ ) and its standard deviation value ( $\sigma_{amine}$ ) were calculated using the following equations:

$$C_{amine} = C_{total,untreated} - C_{total,SNHS-treated}$$
 (7)

$$\sigma_{\text{amine}} = \sqrt{\frac{\sigma_1^2}{n_1} + \frac{\sigma_2^2}{n_2}} \tag{8}$$

where  $\sigma_1$  and  $\sigma_2$  are the standard deviations associated with the total binding sites for biomass samples with and without SNHS treatment, respectively, and  $n_1$  and  $n_2$  represent the number of titrations conducted for the corresponding samples. A P value  $>\!0.05$  was taken to indicate no significant difference between the signals from the biomass or resin samples with and without SNHS treatment. In these cases, the concentration of amine sites in the biomass was too low to be detectable using our approach.

#### **Results and Discussions**

#### 3.1. Titration of a Model Amine compound

In order to demonstrate the ability of our approach to detect amine sites in the expected concentration range of the bacteria and the resin experiments, we conducted titrations of 0.1 M NaCl with and without (blank) 1 mM of CYS (and hence with 1 mM and 0 mM amine sites, respectively) in a pH range of 3.0-9.7. The titration curves show that the 1 mM CYS solution has a significantly stronger buffering capacity above approximately pH 7.5 than the blank solution (Fig. 1). A CYS molecule has three functional groups: carboxyl, amine and sulfhydryl groups, with p $K_a$  values of 1.92, 8.37 and 10.70, respectively (O'Neil, 2013). Therefore, the buffering capacity of the 1 mM CYS solution that we observe from pH 7.5 to 9.7 is primarily due to the deprotonation of the amine group, and our results indicate that the potentiometric titration approach is capable of detecting amine sites in a solution with a concentration of 1 mM. Because deprotonation of the amine sites occurs only within the pH range of 7.0-9.7, we use data from that pH range only to calculate the total amine site concentration of the sample. A one-

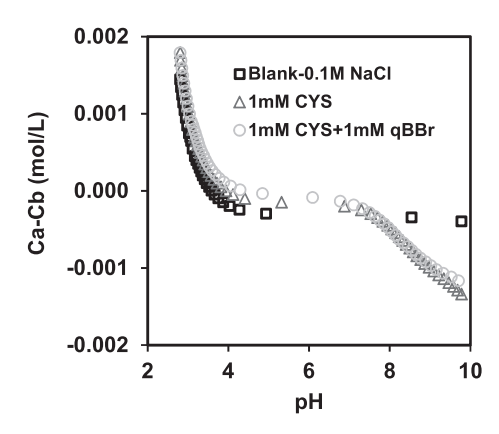


**Fig. 1.** Representative potentiometric titration curves for a blank solution (0.1 M NaCl), a solution with 1 mM CYS in 0.1 M NaCl, and a solution with 1 mM CYS + 1 mM qBBr in 0.1 M NaCl. Triplicates were conducted for each solution, but only one of each type of titration is shown for clarity. The measured concentrations of total sites are 1.04  $\pm$  0.04 mM with a pKa of 8.58  $\pm$  0.01 for the 1 mM CYS solution and 1.04  $\pm$  0.07 mM with a pKa of 8.35  $\pm$  0.02 for the 1 mM CYS + 1 mM qBBr solution.

site model yields a good fit to the 1 mM CYS solution titration data, and the calculated total site concentration is 1.04  $\pm$  0.04 mM with a calculated pKa value of 8.58  $\pm$  0.01 (n = 3). These results are in good agreement with the expected values of 1.00 mM of amine sites, and a pKa of 8.37, for a 1 mM CYS solution (O'Neil, 2013). In contrast, models fail to converge for the titration data for the blank solution, indicating a lack of proton-active sites in the sample.

Although the buffering behavior in the pH range of 7.0-9.7 is dominated by the amine site deprotonation, deprotonation of the sulfhydryl group with a p $K_a$  value of 10.70 may contribute as well in the pH ranged studied. In order to fully account for the contribution of the sulfhydryl group, we conducted additional titration experiments using a 1 mM CYS solution with 1 mM qBBr. qBBr selectively and irreversibly binds to sulfhydryl sites (Kosower and Kosower, 1995; Joe-Wong et al., 2012; Yu et al., 2014), therefore the presence of qBBr causes the sulfhydryl site on the CYS molecule to be blocked for protonation/deprotonation during the titration experiments, and the buffering capacity of the 1 mM CYS + 1 mM qBBr solution in the pH range 7.0–9.7 is due to the amine sites exclusively. As shown in Fig. 1, the titration curve of the 1 mM CYS + 1 mM qBBr is similar to that of the 1 mM CYS alone except at the highest pH values of the titration where the solution with qBBr exhibits a slightly lower buffering capacity. Modeling of triplicate titrations yields an average total site concentration for the 1 mM CYS + 1 mM qBBr solution of 1.04  $\pm$  0.07 mM, still within experimental error of the expected 1 mM of amine sites in the 1 mM CYS solution. Note that the calculated p $K_a$  value for the 1 mM CYS solution changes from 8.58  $\pm$ 0.01 for the qBBr-free solutions, to 8.35  $\pm$  0.02 for the solutions with sulfhydryl sites blocked, a value that agrees perfectly with the reported  $pK_a$  value (8.37) for amine sites on the CYS molecule (O'Neil, 2013). This result further demonstrates that the potentiometric titration and modeling approach coupled with the use of site-specific blocking molecules can accurately and precisely characterize  $pK_a$  values and site concentrations of proton-active sites at least down to 1 mM levels.

Measured total site concentrations on bacterial cell surfaces are typically 0.3–0.5 mmol per gram of wet biomass (Fein et al., 1997; Cox et al., 1999; Ngwenya et al., 2003; Yu et al., 2014). Therefore, if we conduct potentiometric titration experiments using bacterial suspensions with 30–50 g wet biomass/L, the bacterial suspensions would contain 10–25 mM of total sites. Assuming that the amine sites represent at least 10% of the total binding sites on the cell surface, their concentrations should be at least 1 mM and therefore detectable using this approach as long as all of the amine sites are selectively and irreversibly blocked.

#### 3.2. Reaction between SNHS and Non-Amine Sites

In order to test the selectivity of the SNHS amine blocker, we conducted titration experiments using two silica-based resins: a Si-carboxyl resin and a Si-thiol resin, the former was coated with carboxyl groups and the latter was coated with sulfhydryl groups. As shown in Fig. 2, the titration curves of the two resins each show strong buffering capacity relative to the blanks in their characteristic pH ranges. The Si-carboxyl resin exhibits strong buffering behavior across the entire pH range studied, likely due to the presence of carboxyl sites with a wide range of  $pK_a$  values; in contrast, the Si-thiol resin exhibits strong buffering behavior only above approximately pH 8.5. Each type of resin was treated with an excess of SNHS relative to their expected binding site concentrations, and the measured titration curves for the two types of SNHS-treated resins were identical within experimental uncertainty to the titration curves of the corresponding untreated resins. These results indicate that no proton-active binding sites were blocked in the SNHS treatments of either resin type, and hence that SNHS does not react with either carboxyl or sulfhydryl sites. Although a resin coated with phosphoryl sites is not commercially available and hence could not be tested, phosphate-based buffers have been widely used with SNHS amine blocking applications (Boels et al., 2001; Epstein et al., 2003; Lee-Kwon et al., 2003). The fact that the concentration of phosphate in these studies is several orders of magnitude higher than that of SNHS, and that SNHS still effectively reacts with and blocks amine sites, strongly suggests that SNHS does not react with phosphoryl sites either. Together, these results demonstrate that SNHS does not react with the non-amine sites on bacterial surfaces to a significant extent, and hence is ideally suited to block amine sites on bacterial cell surfaces and to leave the carboxyl, sulfhydryl and phosphoryl sites that are also present on the cell surface unblocked.

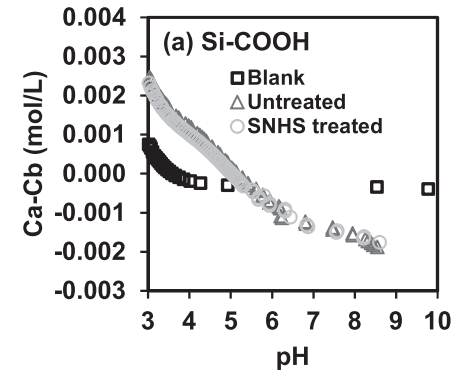
#### 3.3. Reaction between SNHS and Amine Sites

Our preliminary experiments (results not shown) indicated that the unbound SNHS molecule in solution reacts with protons and hence cannot be used to quantify amine site concentrations on aqueous molecules such as cysteine because an excess of unbound SNHS would remain in solution during the titration. However, we tested the reactivity between SNHS and two resins that were coated with different ratios of primary:secondary amine groups. In these experiments, because excess SNHS is removed from the system by washing after treatment of the solids, there are no unbound SNHS molecules in the titration experiments, and the only SNHS molecules that are present during the titrations are those bound onto resin surface amine sites. Our results demonstrate that SNHS readily binds to and blocks the amine sites on both types of resins. As shown in Fig. 3, both resin types exhibit little buffering capacity below pH 5, weak buffering behavior from

approximately pH 5–8, and strong buffering capacity above pH 8. The buffering behavior above pH 8 is likely due to the presence of abundant amine sites on the resin surfaces, and we note that the buffering capacities of the two amine-coated resins are much greater than those that we measured for the Si-carboxyl resin or the Si-thiol resin (Fig. 2). Each molecule grafted onto the amine resins contains three amine sites but the molecules coating the Si-carboxyl and Si-thiol resins contain only one site each, leading to the stronger buffering behavior that we measured for the amine resins.

After the two amine resins were treated with SNHS to block their surface amine sites, the buffering capacity of each type of resin dropped significantly, indicating that amine sites on the two types of resins were blocked successfully by SNHS. However, the titration curves of the two SNHS-treated resins are still significantly different from the titration curve of the blank, and still exhibit a weak buffering capacity, indicating that some proton-active sites are still available on each type of SNHStreated resin. To quantify the total sites on each resin, we attempted to use surface complexation models with different numbers of types of sites to fit the data, and we found that a two-site SCM yields the best fit to the titration curves of both untreated and SNHS-treated amine resins. After SNHS treatment, the concentration of total sites on the SitrisamineB resin decreased from 1.23  $\pm$  0.01 mmol/g to 0.33  $\pm$  0.02 mmol/g, and that on the Si-trisamineS resin decreased from  $1.09\pm0.02$ mmol/g to 0.28  $\pm$  0.04 mmol/g, yielding amine site concentrations on the Si-trisamineB and Si-trisamineS resins of 0.90  $\pm$  0.02 and 0.81  $\pm$ 0.04 mmol/g, respectively (Table 2).

Because uncoated silica surfaces themselves contain proton-active sites, it is possible that the remaining proton-active sites that are available on the SNHS-treated resins are located on the silica structure of the resins. In order to test this hypothesis, and because uncoated silica resins are not available commercially, we conducted potentiometric titration experiments using a Si-sulfonic resin whose sulfonic sites have a  $pK_a < 2$ . Because of such a low  $pK_a$  value, sulfonic sites are virtually all deprotonated over the entire pH range of our experiments, and thus the titration curve for this resin represents a measure of the protonation behavior of the silica surface without any contribution from the sulfonic sites that coat the surface. As shown in Fig. 3, the titration curve of the Si-sulfonic resin is similar to those of the SNHS-treated amine resins, suggesting that the remaining sites on the SNHS-treated amine resins are primarily those located on the silica foundation of the resins. The fitting results further confirm this conclusion as the total concentration of sites on the Si-sulfonic resin is not significantly different from the total site concentrations on either of the SNHS-treated amine resins (Table 2). These results suggest that the sites on the amine resins that remain unblocked after SNHS treatment are located on the silica surface, and that SNHS effectively blocks all of the amine sites on both types of resins. Although the ability for SNHS to bind to primary amines (-NH2) has been well documented (McGee et al., 2012; Mentinova et al., 2012), it was



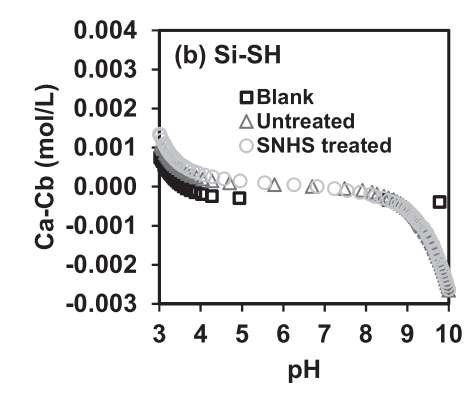
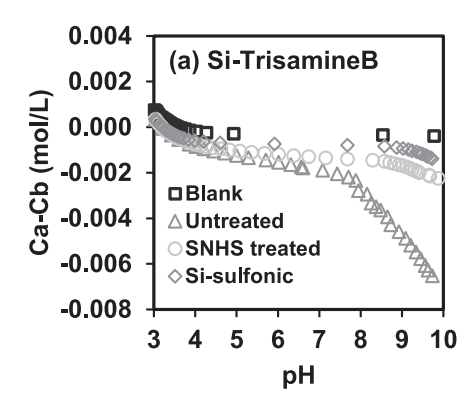


Fig. 2. Potentiometric titration curves for: (a) the untreated and SNHS treated Si-carboxyl resin; (b) untreated and SNHS treated Si-thiol resin. The blank is a 0.1 M NaCl solution and all the resins (5 g/L) were suspended in 0.1 M NaCl solutions. The depicted titration data are from one of the triplicate titrations conducted for each system.



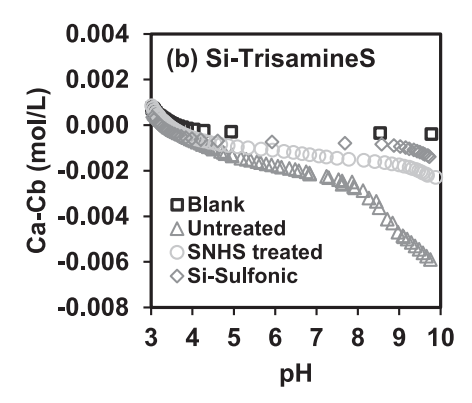


Fig. 3. Representative potentiometric titration curves for: (a) the untreated and the SNHS treated Si-TrisamineB resin; (b) the untreated and the SNHS treated Si-TrisamineS resin. The blank is a 0.1 M NaCl solution and all the resins (5 g/L) were suspended in 0.1 M NaCl solutions. Triplicates were conducted for each solution, but only one of each type of titration is shown for clarity. The titration curve for the Si-sulfonic resin is used for estimating the buffering capacity of the silicate backbone of the Si-Trisamine resins (see text).

unknown whether SNHS reacts with secondary amines (-NH). The two trisamine resins that we studied each contain both primary and secondary amine sites but with different ratios of the two types (Table 1). The fact that all amine sites were blocked by SNHS on each type of amine resin that we tested clearly indicates that SNHS can bind with both primary and secondary amines. Therefore, these results demonstrate that our approach combining selective amine blocking, potentiometric titration and surface complexation modeling yields a total concentration of both the primary and second amine sites on the resin surface.

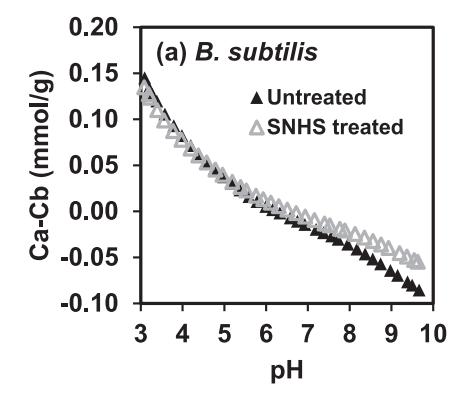
#### 3.4. Measurement of Amine Sites on Bacterial Samples

We used our approach to measure the concentration of total amine sites on the cell surface of one Gram-positive bacterial species, B. subtilis, and one Gram-negative bacterial species, P. putida. As shown in Fig. 4, the buffering capacity of the two biomass samples decreases significantly above approximately pH 6 after the amine sites were blocked by SNHS treatment of each biomass, indicating that each type of bacterial cell contains a measurable concentration of amine sites on their cell surfaces. The pH range where the decrease in buffering capacity is most evident is consistent with the reported  $pK_a$  values of amine sites on small molecules, further demonstrating the effectiveness in blocking amine sites using a SNHS treatment. Fig. 4 also shows that the buffering capacity of P. putida decreases more than that of B. subtilis after amine sites are blocked, suggesting that the P. putida cell surface contains a higher concentration of surface amine sites than that of B. subtilis.

As was found in previous studies involving potentiometric titrations of bacterial biomass (Fein et al., 1997; Yu et al., 2014), a four-site non-electrostatic surface complexation model is required to fit the titration data of all the untreated biomass samples in this study, each of the three

titrations of the SNHS-treated B. subtilis biomass samples, and one of the three titrations of the P. putida biomass (Table 3). Two of the three titration curves for the SNHS-treated P. putida biomass required fewer sites to account for the observed decreased buffering behavior, with one requiring a two-site and one requiring a three-site model. The decreased number of site types required to model the buffering behavior of the SNHS-treated P. putida titrations is likely a result of the lower concentration of proton-active sites on the SNHS-treated P. putida compared to the other biomass samples. Although models with different number of sites were required to fit each of the triplicate titrations for the SNHStreated P. putida sample, the calculated total site concentrations for the three different SNHS-treated P. putida titrations are relatively consistent, ranging from 160 to 179 µmol/g (Table 3). The fact that the SNHS treatment does not simply eliminate one of the  $pK_a$  values but rather it decreases more than one of the individual site concentrations (Table 3) reinforces our understanding that a specific  $pK_a$  value from our modeling approach does not correspond to only one type of chemical binding site moiety. That is, not all amine (or carboxyl, phosphoryl, sulfhydryl, etc.) sites deprotonate with the same  $pK_a$  value, and not all sites that deprotonate with the same  $pK_a$  value are of a specific site type chemically.

After we blocked the amines sites on the bacterial cells, the average measured total site concentration for *B. subtilis* decreased from  $220\pm1$  to  $168\pm9$  µmol/g, and that for *P. putida* decreased from  $245\pm4$  to  $171\pm10$  based on triplicate titrations. The decreases are statistically significant (P<0.05, Table 4), and therefore represent the concentration of total amine sites on each biomass sample. For *B. subtilis*, the concentration of total amine sites is  $52\pm5$  µmol/g and accounts for  $\sim24\%$  of the total proton-active binding sites on the cell surface. The calculated amine site concentration for *P. putida* is  $78\pm6$  µmol/g and accounts for



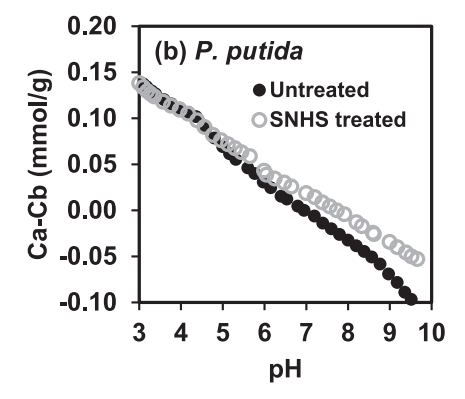


Fig. 4. Representative potentiometric titration curves for the untreated and SNHS-treated biomass samples of: (a) *B. subtilis* and (b) *P. putida*. Each biomass suspension contains 30 g/L of bacterial cells and 0.1 M NaCl. Triplicates were conducted for each solution, but only one of each type of titration is shown for clarity.

**Table 3**Binding site concentrations on untreated and SNHS-treated biomass samples.

Sample	pK <sub>a, 1</sub>	pK <sub>a, 2</sub>	pK <sub>a, 3</sub>	pK <sub>a, 4</sub>	Site1	Site2	Site3	Site4	Total
					μmol/g	μmol/g	μmol/g	μmol/g	μmol/g
BS	3.8	5.4	7.5	9.1	$81.2 \pm 0.9$	$52.9 \pm 2.4$	$34.9 \pm 0.5$	$50.5\pm1.3$	$219.5\pm0.7$
SNHS-BS	3.9	5.6	7.4	9.1	$68.0\pm1.4$	$38.1 \pm 8.7$	$27.0\pm0.3$	$35.0\pm1.7$	$168.0\pm8.7$
PP	5.0	6.4	7.8	9.5	$77.4 \pm 5.3$	$36.6 \pm 3.5$	$46.7 \pm 7.2$	$83.9 \pm 5.4$	$244.6 \pm 3.5$
SNHS-PP #1	6.0	8.6			101.1	59.4			160.4
SNHS-PP #2	4.7	5.9	7.8	9.3	43.1	47.4	43.8	39.6	173.8
SNHS-PP #3	4.8	6.7	8.8		72.1	56.7	50.3		179.2

BS = B. *subtilis* (the average values from triplicate titrations are shown).

PP = P. *putida* (the results from each triplicate titration are shown).

Reported uncertainties are  $1\sigma$  values based on triplicate experiments.

**Table 4**Total site and amine site concentrations on *Bacillus subtilis* and *Pseudomonas putida*.

Bacterium	Treatment	Total Sites*	P value#	Amine Sites*	
		μmol/g		μmol/g	
B. subtilis	untreated	$220\pm1$	0.014	52 ± 5	
D. SUDUUS	SNHS-treated	$168 \pm 9$	0.014		
P. putida	untreated	$244\pm4$	0.002	$78\pm 6$	
	SNHS-treated	$167\pm10$	0.002		

 $<sup>^{^*}</sup>$  Values are average measured concentrations and  $1\sigma$  uncertainties based on triplicate experiments for each condition.

 $\sim$ 32% of total sites on the *P. putida* cell surface, significantly higher values than the value that we measured for B. subtilis. The concentration of sulfhydryl sites on B. subtilis and P. putida cells that grew under the same conditions to those in this study is 23  $\pm$  7  $\mu$ mol/g and 35  $\pm$  10 μmol/g, respectively (Yu et al., 2014; Yu and Fein, 2016), less than half of the concentration that we measured here for amine sites. Although we do not know the specific concentrations of carboxyl or phosphoryl sites on the surfaces of these two bacterial species, the concentration of amine sites on the cell surface of these bacterial species is at least comparable with that of carboxyl and phosphoryl sites given that the amine sites account for 24-32% of total sites on each type of cell surface. This is the first study to quantify the absolute and relative abundances of amine sites on bacterial cell surfaces. The results clearly indicate that amine sites do not represent a minor component of the overall range of binding sites on at least these two types of bacterial surfaces, but rather that they are present in abundance and likely play a significant role in the binding and the bioavailability of anionic aqueous species.

In order to fully understand the role of amine sites in bacteriallymediated processes, it will be crucial to extend this study to measure amine site concentrations on other bacterial species and on cells from other growth conditions. Our study verifies the selectivity and irreversibility of SNHS binding onto amine sites in general, and provides the first measurements of amine site concentrations on undisturbed bacterial cell surfaces. The approach of selectively blocking microbial cell surface amine binding sites using SNHS can be useful in probing the contribution of amine sites to a range of microbe-contaminant interactions such as bacterial cell surface adsorption and reduction of anionic contaminants (Yu et al., 2018; Butzen and Fein, 2020; Brown et al., 2024). A better understanding of the concentration and roles of bacterial cell surface amine sites will yield more accurate models of the fate and transport of contaminants in the environment, and will aid in the development of more effective and efficient remediation approaches for contaminated waters and soils.

#### CRediT authorship contribution statement

**Qiang Yu:** Writing – review & editing, Writing – original draft, Visualization, Project administration, Methodology, Investigation, Formal analysis, Data curation, Conceptualization. **Jeremy B. Fein:** Writing – review & editing, Supervision, Project administration, Funding acquisition, Conceptualization.

#### **Declaration of competing interest**

The authors declare the following financial interests/personal relationships which may be considered as potential competing interests: Jeremy B. Fein reports financial support was provided by US National Science Foundation. If there are other authors, they declare that they have no known competing financial interests or personal relationships that could have appeared to influence the work reported in this paper.

#### Data availability

Data will be made available on request.

#### Acknowledgements

QY was supported through the Center for Environmental Science and Technology at University of Notre Dame. The research was funded in part by U.S. National Science Foundation grant EAR-2149717. Two journal reviews were thorough and helped improve the presentation of the research.

#### References

Beveridge, T.J., Murray, R.G.E., 1976. Uptake and Retention of Metals by Cell Walls of bacillus Subtilis. J. Bacteriol. 127 (3), 1502–1518.

Beveridge, T.J., Murray, R.G.E., 1980. Sites of Metal Deposition in the Cell Wall of bacillus Subtilis. J. Bacteriol. 141 (2), 876–887.

Boels, K., et al., 2001. The neuropeptide head activator induces activation and translocation of the growth-factor-regulated Ca2+-permeable channel GRC. J. Cell Sci. 114 (20), 3599–3606.

Brown, J.C., Mackay, Q., Yu, Q., Fein, J.B., 2024. The role of cell surface sulfhydryl and amine binding sites in the reduction of Cr(VI) from solution by Bacillus subtilis bacterial cells. Chemical Geology (under review).

Butzen, M.L., Fein, J.B., 2020. Electron Donor Effects on Bacterial Surface Sulfhydryl Site Concentrations. Geomicrobiol J. 1–10.

Chang, E., Lammers, L.N., Pallud, C., 2023. High-affinity amide-lanthanide adsorption to gram-positive soil bacteria. Environ. Microbiol. Rep. 15 (5), 417–421.

Cox, J.S., Smith, D.S., Warren, L.A., Ferris, F.G., 1999. Characterizing heterogeneous bacterial surface functional groups using discrete affinity spectra for proton binding. Environ. Sci. Technol. 33 (24), 4514–4521.

Daughney, C.J., Fein, J.B., 1998. The effect of ionic strength on the adsorption of H<sup>+</sup>, Cd<sup>2</sup>

<sup>+</sup>, Pb<sup>2+</sup>, and Cu<sup>2+</sup> by *Bacillus subtilis* and *bacillus licheniformis*: a surface complexation model. J. Colloid Interface Sci. 198 (1), 53–77.

Daughney, C.J., Siciliano, S.D., Rencz, A.N., Lean, D., Fortin, D., 2002. Hg(II) adsorption by bacteria: a surface complexation model and its application to shallow acidic lakes and wetlands in Kejimkujik National Park, Nova Scotia, Canada. Environmental Science & Technology 36 (7), 1546–1553.

Deng, S., et al., 2008. Enhanced Adsorption of Arsenate on the Aminated Fibers: Sorption Behavior and Uptake Mechanism. Langmuir 24 (19), 10961–10967.

 $<sup>^{\#}</sup>$  P values were obtained from the Student's *t*-test for the total site concentrations of the untreated and SNHS-treated biomass samples.

- Deng, S., Ma, R., Yu, Q., Huang, J., Yu, G., 2009. Enhanced removal of pentachlorophenol and 2,4-D from aqueous solution by an aminated biosorbent. J. Hazard. Mater. 165 (1), 408–414.
- Deng, S., et al., 2013. Adsorption of perfluorinated compounds on aminated rice husk prepared by atom transfer radical polymerization. Chemosphere 91 (2), 124–130.
- Epstein, A.L., Mizokami, M.M., Li, J., Hu, P., Khawli, L.A., 2003. Identification of a Protein Fragment of Interleukin 2 responsible for Vasopermeability. JNCI J. Natl. Cancer Inst. 95 (10), 741–749.
- Eßmann, R., 1995. Influence of coordination on N·H···X— hydrogen bonds. Part 1. [Zn (NH3)4]Br2 and [Zn(NH3)4]I2. J. Mol. Struct. 356 (3), 201–206.
- Fein, J.B., Daughney, C.J., Yee, N., Davis, T.A., 1997. A chemical equilibrium model for metal adsorption onto bacterial surfaces. Geochim. Cosmochim. Acta 61 (16), 3319–3328.
- Fein, J.B., Boily, J.-F., Yee, N., Gorman-Lewis, D., Turner, B.F., 2005a. Potentiometric titrations of *Bacillus subtilis* cells to low pH and a comparison of modeling approaches. Geochim. Cosmochim. Acta 69 (5), 1123–1132.
- Fein, J.B., Boily, J.F., Yee, N., Gorman-Lewis, D., Turner, B.F., 2005b. Potentiometric titrations of Bacillus subtilis cells to low pH and a comparison of modeling approaches. Geochim. Cosmochim. Acta 69 (5), 1123–1132.
- Fuchs, G., Boll, M., Heider, J., 2011. Microbial degradation of aromatic compounds from one strategy to four. Nat. Rev. Microbiol. 9 (11), 803–816.
- Guiné, V., et al., 2006. Zinc sorption to three Gram-negative bacteria: combined titration, modeling, and EXAFS study. Environ. Sci. Technol. 40 (6), 1806–1813.
- Jiang, W., et al., 2004. Elucidation of functional groups on Gram-positive and Gramnegative bacterial surfaces using infrared spectroscopy. Langmuir 20 (26), 11433-11442.
- Joe-Wong, C., Shoenfelt, E., Hauser, E.J., Crompton, N., Myneni, S.C.B., 2012. Estimation of Reactive Thiol Concentrations in Dissolved Organic Matter and Bacterial Cell Membranes in Aquatic Systems. Environ. Sci. Technol. 46 (18), 9854–9861.
- Kang, F.X., Qu, X.L., Alvarez, P.J.J., Zhu, D.Q., 2017. Extracellular Saccharide-Mediated Reduction of Au3+ to Gold Nanoparticles: New Insights for Heavy Metals Biomineralization on Microbial Surfaces. Environ. Sci. Technol. 51 (5), 2776–2785.
- Kosower, E.M., Kosower, N.S., 1995. [12] Bromobimane probes for thiols, Methods in Enzymology. Academic Press, pp. 133–148.
- Lee-Kwon, W., Kawano, K., Choi, J.W., Kim, J.H., Donowitz, M., 2003. Lysophosphatidic Acid Stimulates Brush Border Na<sup>+</sup>+</sup> +</sup> Exchanger 3 (NHE3) activity by increasing its Exocytosis by an NHE3 Kinase a Regulatory Protein-dependent Mechanism \*. J. Biol. Chem. 278 (19), 16494–16501.
- Lovley, D.R., 1993. Dissimilatory Metal Reduction. Annu. Rev. Microbiol. 47, 263–290.
   McGee, W.M., Mentinova, M., McLuckey, S.A., 2012. Gas-phase Conjugation to Arginine Residues in Polypeptide Ions via N-Hydroxysuccinimide Ester-based Reagent Ions.
   J. Am. Chem. Soc. 134 (28), 11412–11414.

- Mentinova, M., Barefoot, N.Z., McLuckey, S.A., 2012. Solution Versus Gas-phase Modification of Peptide Cations with NHS-Ester Reagents. J. Am. Soc. Mass Spectrom. 23 (2), 282–289.
- Mishra, B., McDonald, L.M., Roy, M., Lanzirotti, A., Myneni, S.C.B., 2020. Uptake and speciation of zinc in edible plants grown in smelter contaminated soils. PloS One 15 (4), e0226180.
- Modec, B., Podjed, N., Lah, N., 2020. Beyond the simple copper(II) Coordination Chemistry with Quinaldinate and secondary Amines. Molecules 25 (7), 1573.
- Ngwenya, B.T., Sutherland, I.W., Kennedy, L., 2003. Comparison of the acid-base behaviour and metal adsorption characteristics of a Gram-negative bacterium with other strains. Appl. Geochem. 18 (4), 527–538.
- O'Neil, M.J., 2013. The Merck Index: An Encyclopedia of Chemicals, Drugs, and Biologicals. Encyclopedia of Chemicals, Drugs, and Biologicals. Royal Society of Chemistry, Cambridge, UK.
- Pagnanelli, F., Papini, M.P., Toro, L., Trifoni, M., Veglio, F., 2000. Biosorption of metal ions on *Arthrobacter sp.*: Biomass characterization and biosorption modeling. Environ. Sci. Technol. 34 (13), 2773–2778.
- Srinath, T., Verma, T., Ramteke, P.W., Garg, S.K., 2002. Chromium (VI) biosorption and bioaccumulation by chromate resistant bacteria. Chemosphere 48 (4), 427–435.
- Takahashi, Y., Chatellier, X., Hattori, K.H., Kato, K., Fortin, D., 2005. Adsorption of rare earth elements onto bacterial cell walls and its implication for REE sorption onto natural microbial mats. Chem. Geol. 219 (1–4), 53–67.
- Tariq, A., Ullah, U., Asif, M., Sadiq, I., 2019. Biosorption of arsenic through bacteria isolated from Pakistan. Int. Microbiol. 22 (1), 59–68.
- ThermoScientific, 2023. Pierce™ Sulfo-NHS-Acetate.
- Westall, J.C., 1982. FITEQL, a Computer Program for Determination of Chemical Equilibrium Constants from Experimental Data. Version 2.0. Report 82-02, Dept. Chem., Oregon St. Univ. Corvallis, OR, USA.
- Xue, H.B., Stumm, W., Sigg, L., 1988. The binding of heavy-metals to algal surfaces. Water Res. 22 (7), 917–926.
- Yee, N., Benning, L.G., Phoenix, V.R., Ferris, F.G., 2004. Characterization of metalcyanobacteria sorption reactions: a combined macroscopic and infrared spectroscopic investigation. Environ. Sci. Technol. 38 (3), 775–782.
- Yu, Q., Fein, J.B., 2016. Sulfhydryl Binding Sites within Bacterial Extracellular Polymeric Substances. Environ. Sci. Technol. 50 (11), 5498–5505.
- Yu, Q., Szymanowski, J., Myneni, S.C.B., Fein, J.B., 2014. Characterization of sulfhydryl sites within bacterial cell envelopes using selective site-blocking and potentiometric titrations. Chem. Geol. 373, 50–58.
- Yu, Q., Boyanov, M.I., Liu, J., Kemner, K.M., Fein, J.B., 2018. Adsorption of Selenite onto Bacillus subtilis: the Overlooked Role of Cell Envelope Sulfhydryl Sites in the Microbial Conversion of Se(IV). Environ. Sci. Technol. 52 (18), 10400–10407.